Supplementary Information

S1. NiO bulk calculations

The NiO in its rock-salt structure with a lattice parameter of 4.168 Å is considered in its antiferromagnetic ordering AFII (stacking of ferromagnetic planes along the [111] direction) [45]. Different effective U values have been considered in the calculation of the exchange couplings, as can be seen in Fig. S1.

A projection approach has been used in the Wannierisation procedure, considering as initial projectors p orbitals for the O and d orbitals for the Ni, in an energy window $\approx [-12, a)$ eV around the Fermi energy, where a is a U-dependent parameter that was modified in order to include the d orbitals at the bottom of the conduction band. No localization iteration has been applied, in order to avoid spurious hybridisation between the p orbitals and d orbitals in the building of the tight-binding hamiltonian.

From the ground state point of view to an increase in U corresponds an increase in the magnetic moment on the Ni, and a respective decrease in charge on the Ni and increase in charge on the O. The noise introduced by the Wannierisation procedure has been evaluated through the fitting with respect to the DFT energy bands. At this point, through the MFT, a mapping between the tight-binding hamiltonian and an isotropic Heisenberg hamiltonian has been considered, obtaining the exchange couplings of the system for different U values; note that spin-orbit coupling associated terms are not significant.

The error on the J values can be qualitatively associated to the noise on the wannierisation as $Err \sim [\eta/(W/N_b)] * [\eta_{max}/t_{max}]$ where W is the energy window opening, N_b the number of Wannier bands, $t_{max}(\ 2eV)$ the maximum band width in the energy window, and η the average noise on the Wannierisation

$$\eta = \sqrt{\frac{1}{N_k} \sum_{mk} (E_{DFT,mk} - E_{Wann,mk})^2} \tag{S1}$$

with the maximum deviation measured as $\eta_{max} = \max_{mk} |E_{DFT,mk} - E_{Wann,mk}|$. As can be observed, the noise on the Wannierisation is quite low for U parameters inside the interval $[4.5, 6.5]$ of major interest. Outside, it can become significant ($> 20\%$), as the parameter of the Wannierisation were optimized for that interval. Nonetheless, we remark that the trend of increasing

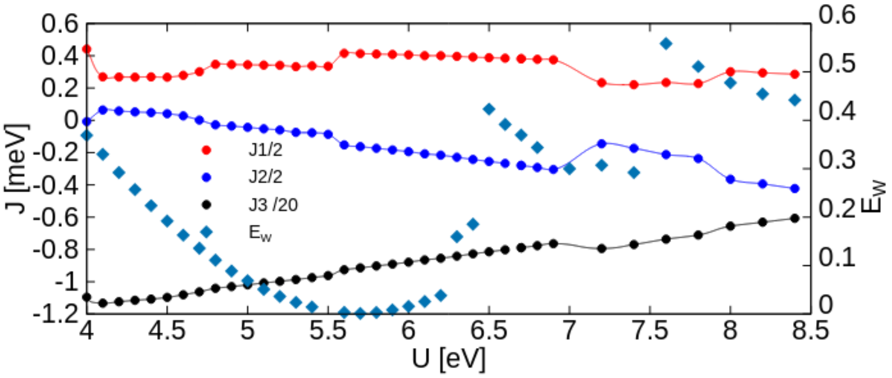

Figure S1: Main exchange couplings in the NiO bulk for different U values: J_1 (red) and J_2 (dark-blue) between Ni atoms along the [111] planes, and J_3 (black) between different [111] planes, through the O atoms. It is reported a qualitative evaluation of the error on the J couplings due to the Wannierisation procedure (light-blue), see Eq. S1 and its discussion.

J_3 with increasing U is smoothly maintained even if η is larger, suggesting a robustness in the procedure.

From the results of Fig. S1, we have selected $U = 5.8$ eV for the Ni atoms, which gives exchange couplings in between the experimental results [21, 30]. The corresponding band structure is reported in Fig. S2.

S2. Additional results from FePc/NiO(001) calculations

Due to the fact that only the Γ point has been considered in the supercell calculations, to evaluate the quality of the Wannierisation we look at the PDOS (an analysis of the band structure is instead performed in the bulk case). The error on the J values as resulting from the Wannierisation procedure is then qualitatively associated to the following definition of a weighted average difference of DFT and Wannier projection:

$$\eta = \sqrt{\sum_i \left(\frac{w_{DFT,i} - w_{Wan,i}}{w_{DFT,i} + w_{Wan,i}} \right)^2} \tag{S2}$$

where $w_i = |\langle \psi_i | A \rangle|^2$ is the projection of the Kohn-Sham states in the energy bin i (0.1eV) over the atomic orbitals of a group of atoms indicated by

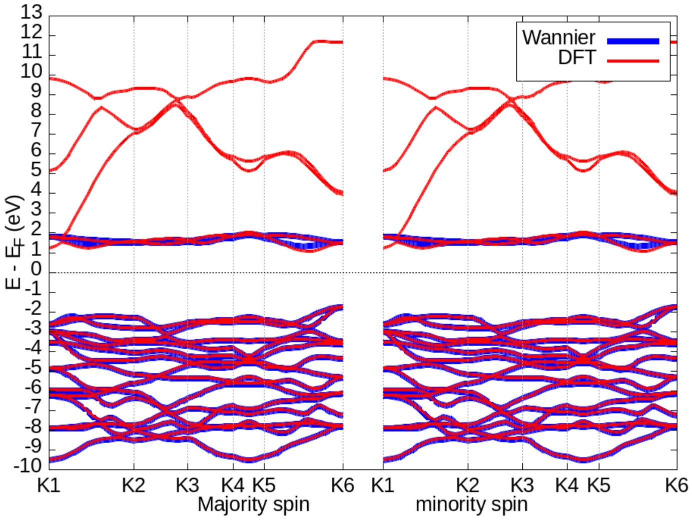

Figure S2: Electronic Band Structure of NiO bulk. Solid/dash-dotted lines indicate DFT and Wannier results, respectively. Spin-up components are shown on the right, while spin-down on the left. The position of the Fermi energy in the gap is arbitrary.

A. In Fig. S3 we report the PDOS from the DFT and the Wannierisation calculations, the different atoms of the molecule have been grouped: C atoms and N atoms. It emerges, for the clean substrate an error of 4%, while for the adsorbed system an error of 7%, which assure us of the quality of the Wannierisation procedure. Moreover, we report in Fig. S4 the charge density and magnetic moment variations in the different layers, used to explain the variations in the exchange couplings due to the molecule adsorption. In particular, the variations of the exchange couplings in the top layer are reported in Fig. S5.

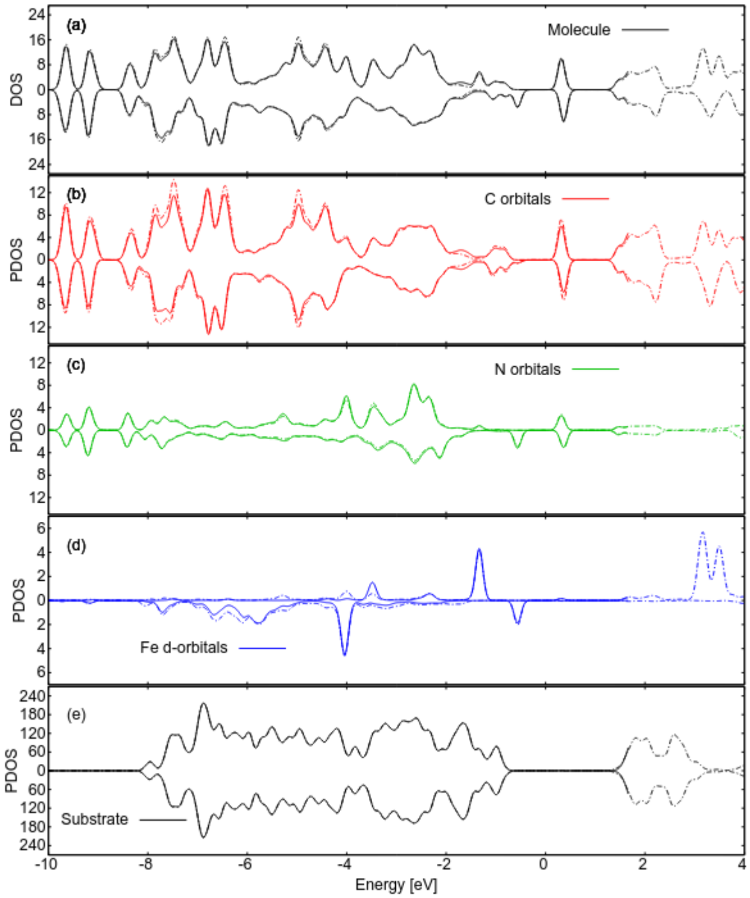

Figure S3: Electronic PDOS of FePc/NiO(001) summed over (a) all molecule atoms; (b) C; (c) N; (d) Fe; (e) substrate atoms. Solid/dash-dotted lines indicate Wannier and DFT results, respectively. Spin-down components are shown as negative values. All values in states/eV/cell. The position of the Fermi energy in the gap is arbitrary.

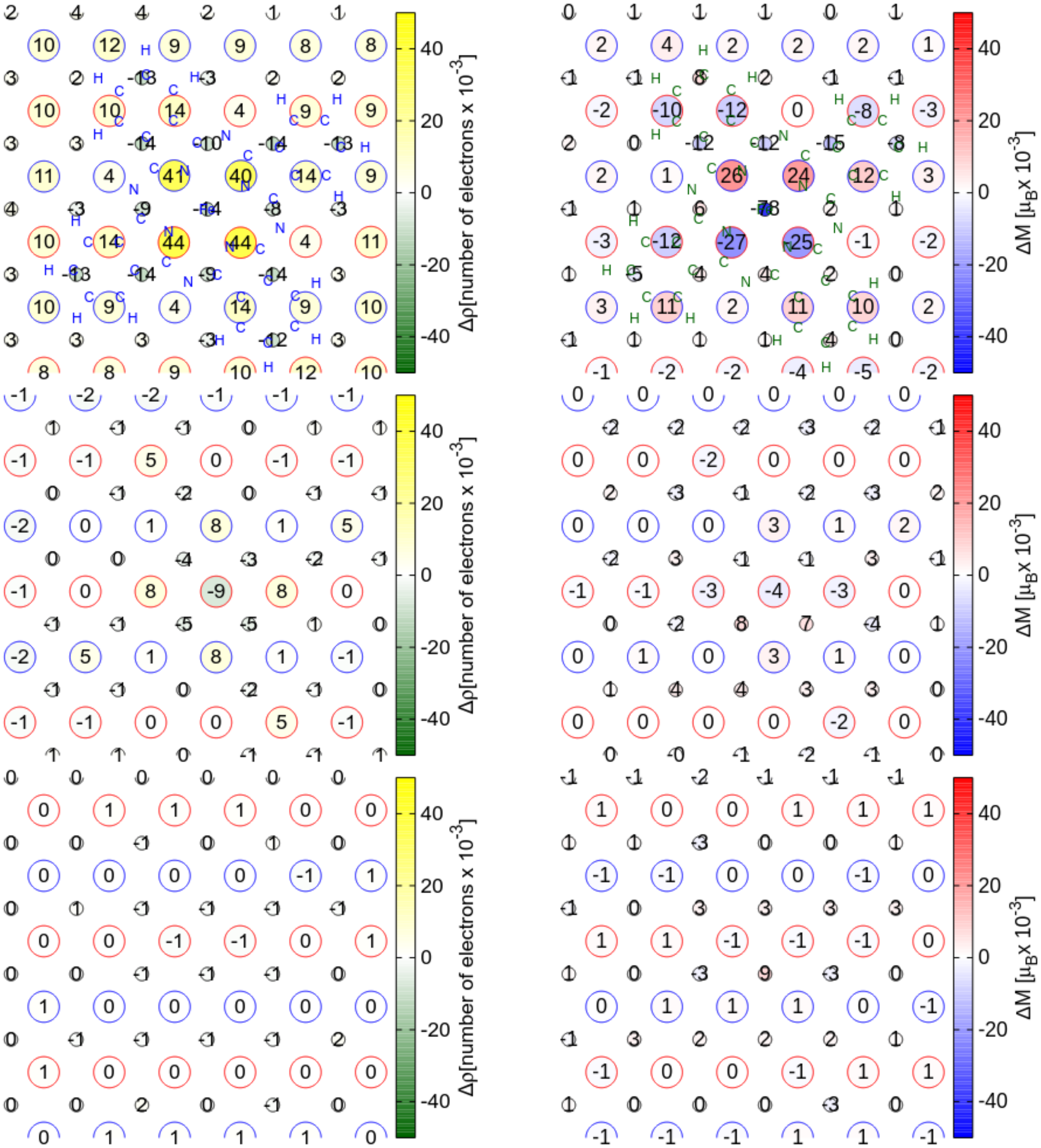

Figure S4: Variations in the electron density (Right) and in the atomic magnetic moments (Left) for the substrate of FePc/NiO(001), with respect to the pristine substrate, for the three layers (top-bottom) (positive = increase in electron population/ in the atomic magnetic moment). The position of the molecule atoms is marked by blue/green letters in the top pannels.

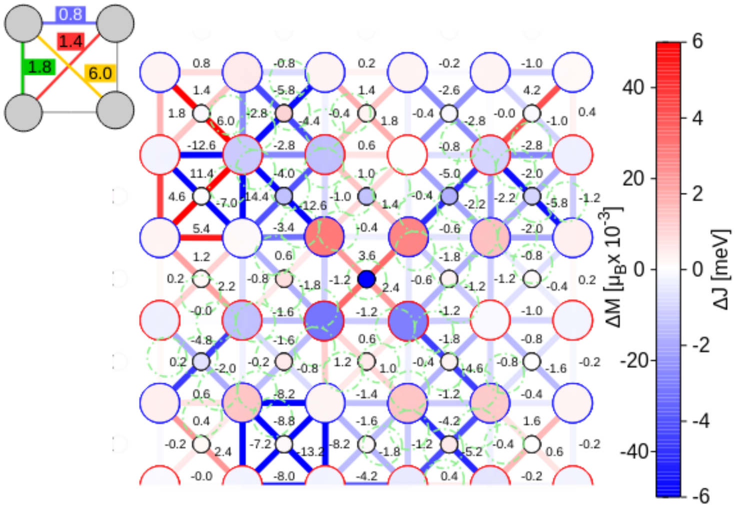

Figure S5: Changes in the exchange couplings ΔJ and in the atomic magnetic moments ΔM of the substrate of FePc/NiO(0001) with respect to the pristine substrate. The position of the molecule atoms is marked by green circles. The circles represent the atoms, the ones with smaller radius the O atoms, while the other ones the Ni atoms; the filling color of each circle is the corresponding variation in the magnetic moment ΔM (the number in the circle quantifies this variation), the color of the contour of each Ni circle represents its initial magnetization before the molecule adsorption. The colored lines between pair of atoms represent the variations in the exchange couplings between the pair ΔJ. The number on the line quantifies the exchange couplings variations as indicated in the inset for a specific unit cell.

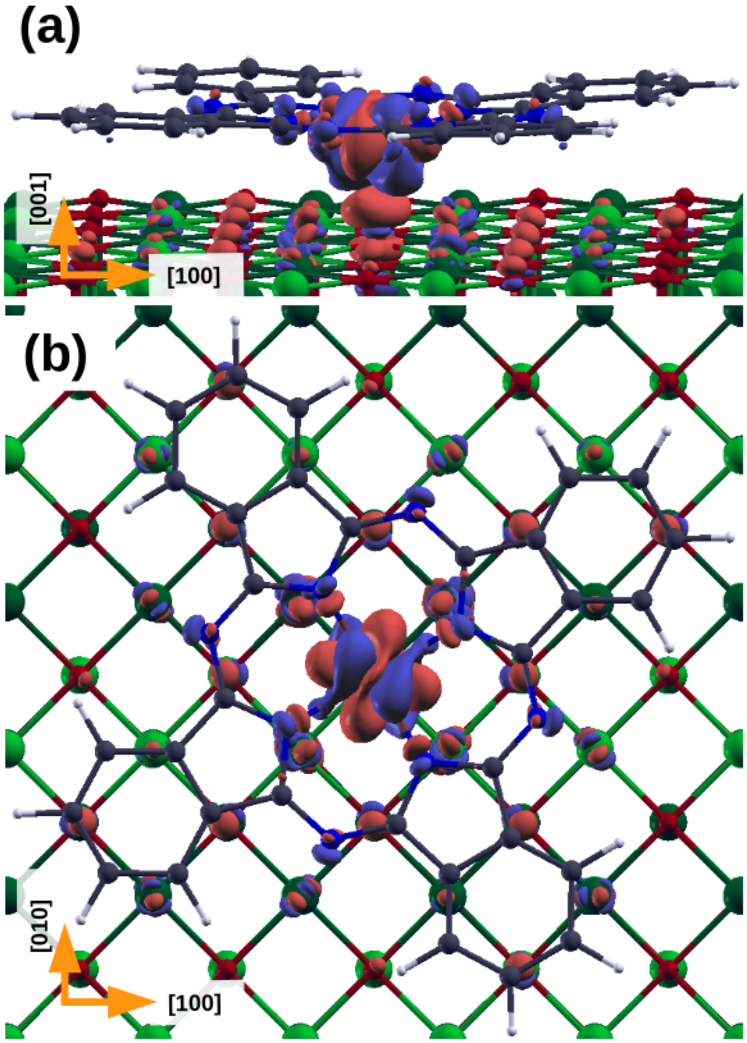

Figure S6: Side-view (a) and top-view (b) of the charge density variations of the minimum energy adsorption configuration with respect to the isolated systems (full-color regions correspond to values whose modulus exceeds 0.003 Å^{-3}). Red/blue: increase/decrease in charge density.

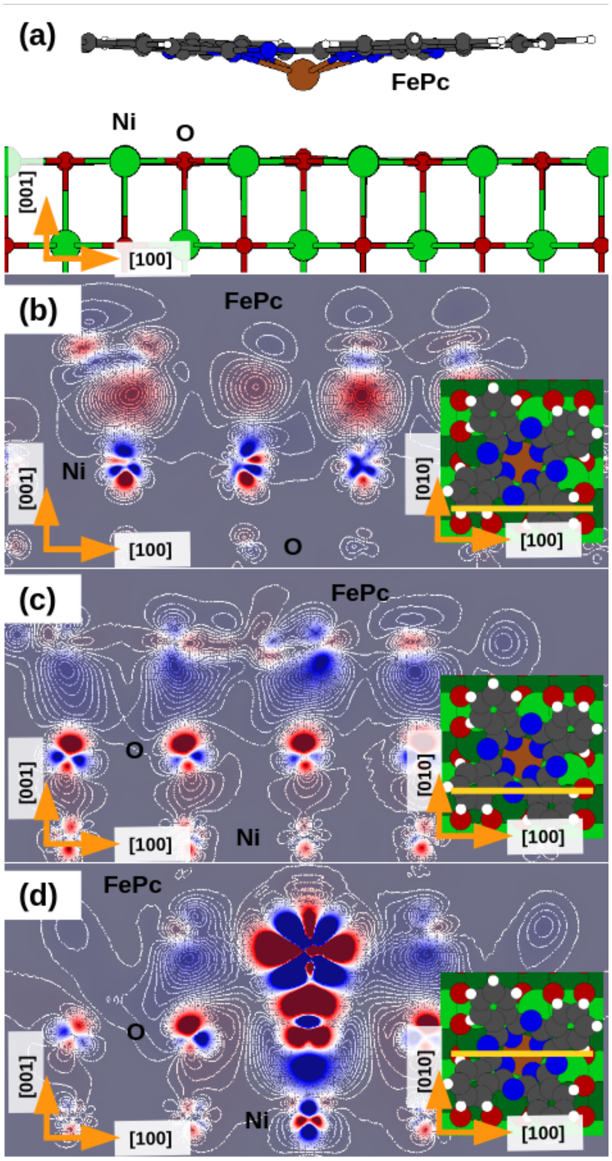

Figure S7: Side-view (b)-(c)-(d) of different cross-sections (as indicated in the left insets) of the charge density variations of the minimum energy adsorption configuration (a) with respect to the isolated systems (full-color regions correspond to values whose modulus exceeds 0.003 Å^{-3}). Red/blue: increase/decrease in charge density.